Algerian Journal of Environmental Science and Technology
December edition. Vol.7. Nº4. (2021)
ISSN : 2437-1114
www.aljest.org

Functionalized mesoporous silica materials for dyes adsorption

A.Barca[1], A. Benhamou[1*], N. Benyoub[1], A. Debab[1]

[1]Laboratoire d'Ingénierie des Procédés de l'Environnement, Département de Génie Chimique, Faculté de Chimie;
Université des Sciences et de Technologie d'Oran Med BOUDIAF, B.P 31015, Oran, Algérie

*Corresponding author: abdellah.benhamou@univ-usto.dz

ARTICLE INFO

Article History:

Received ***:27/01/2020***
Accepted ***:15/07/2020***

***Key Words*:**

Mesoporous materials;
Functionalization;
Dihexylamine;
Adsorption;
Ionic dyes.

ABSTRACT/RESUME

Abstract : *The mesoporous material silica MCM-41 was synthesized under basic media using pure silica, cetyltrimethylammonium bromide and tetramethylammonium hydroxide at 90°C, and then hydrothermally treated by dihexylamine (DHA) at 130°C for 72 h in order to inflate the pores. The post-synthesized material (DHA-41A), the material obtained after selective ethanol extraction of DHA (DHA-41B) and the organic-free material obtained after carbonization of DHA-41A and/or DHA-41B afford (DHA-41C). Small angle X-ray diffraction, nitrogen adsorption–desorption measurements, FT-IR, thermogravimetry and zetametrie were used to characterize all the samples. The samples were evaluated as adsorbent for two dyes Naphtol Green B (NGB) as anionic dye and Rhodamine B (RB) as cationic dye. DHA-41A and DHA-41C were found to be fast adsorbent for the anionic and the cationic dye respectively. Adsorption capacities of NGB onto DHA-41A and RB onto DHA-41C, were found 444.55 and 372.59 mg/g respectively. Adsorption kinetic data were tested using pseudo-first-order and pseudo-second-order models and intraparticle diffusion. Adsorption data were modeled using Langmuir, Freundlich and Sips adsorption isotherms. The result revealed that the adsorption of the anionic dye onto DHA-41A and the cationic dye onto DHA-41C, fitted very well with the Langmuir and Sips isotherm model* than *Freundlich isotherm model.*

I. Introduction

Dyes represent an important class of dangerous compounds, since the discharge of dye-bearing wastewater into natural streams and rivers from textile, paper, carpet, leather, distillery, and printing industries affects both the life of aquatic organisms and human health, [1]. Dyes are not only toxic but they change the color of the water, [2, 3]. Different techniques such as coagulation, flocculation, membrane, chemical oxidation, adsorption, precipitation, and photo/biological degradation were used to remove dyes from water. However, amongst all the aforementioned techniques, adsorption is considered to be the most convenient and effective method for remediation owing to its high efficiency, simplicity and cost feasibility [4]. A large number of adsorbents such as zeolites, activated carbon, resins, fly ash, chitosan and others are used for the removal of heavy metals, dyes and other pollutants from wastewater. Activated carbon is the most extensively used adsorbent for the removal of pollutants from wastewater due to its high surface area, stability and durability [5]. The expensive synthesis and difficult regeneration limit its application in large scale wastewater treatment **[6].** Among a variety of adsorbents, ordered mesoporous silicas are very interesting and versatile materials because of their high surface area, uniform pore size distribution, and easy surface functionalization. All these features, together with a low production cost, constitute primary advantages

of ordered mesoporous silica respect to other materials with high pollutants adsorption capacities [7]**.** In the design of improved MCM-41 for the adsorption of specific substance, surface installation and operating cost. modification is very helpful in the improvement of the adsorption capacity and selectivity of MCM-41 by taking advantage of specific interactions between the adsorbents and the adsorbates [8-10]. The present study is concerned with the preparation and modification of the surface of MCM-41 for dye adsorption application. MCM-41 has been undergone by various modifications in which the resulting materials have been used as adsorbents for dyes removal. The different materials were tested to remove two different dyes (anionic dye Naphtol Green B (NGB) and cationic dye Rhodamine B (RB)). The adsorption isotherms and kinetics of the adsorbents were measured. Equilibrium data were fitted to Langmuir and Freundlich equations to determine the correlation between the isotherm models and experimental data.

II. Materials and methods

II.1 Preparation of MCM-41

Mesoporous silica MCM-41 was synthesized according to the procedures described in the literature, [11, 12] using cetyltrimethyammonium bromide (CTAB), tetramethylammonium hydroxide (TMAOH) and fumed silica source. The molar ratio is: 1 SiO_2; 0.45 CTAB; 0.32 TMAOH; 67 H_2O. Firstly, the solution of TMAOH and CTAB was prepared using deionized water, and then the silica source was added with stirring for 2 hours at room temperature. The gel was text actually exist hydrothermally treated at 373 K for 48 hours. Finally, the obtained product was recovered by filtration, washed with deionized water, and dried under ambient conditions.

II.2 Functionalization by Amines

The surface functionalization was achieved through post-synthesis treatment. Firstly, 5g of the as-synthesized material MCM-41 was added to the solution containing 7g of dihexylamine (DHA) and 78 mL of distilled water under magnetic stirring for 30 min. The mixture was hydrothermally treated at 393K for 72 hours. The product was recovered by filtration, washed several times with distilled water, and dried. The material was denoted DHA-41A. The amine was extracted by soxhlet using ethanol and dried under ambient conditions. The new material was denoted DHA-41B. Calcinations of materials A or B affords material denoted DHA-41C.

II.3 Adsorbates and Characterization

NGB and RB dyes were selected as adsorbates to discuss the adsorption selectivity and capacity of as-synthesized MCM-41 and its modified counterparts. NGB dye was purchased from Alfa Aesar A Johnson Matthey Company (US) and RB dye was purchased from BIOCHEM Chemopharma (Quebec), the both dyes were used without further purification.

Nitrogen adsorption-desorption isotherms was measured by a Micromeritics ASAP 2000 and ASAP 2010 at 77 K. The specific surface area (SSA) was determined using the Brunauer–Emmett–Teller method. The pore diameter was calculated by using the adsorption branch of the isotherm [13]. The pore distribution was obtained by the method of Barett et al. [14]. The structure of all samples was determined by X-ray diffraction (XRD) recorded on a Brucker AXS D-8 X-ray powder diffractometer (Cu Kα radiation, k = 1.5418 Å). The thermal properties of all samples were determined by thermogravimetric analysis obtained on a Model TGA 2950 high-resolution thermogravimetric analyzer NETZSCH Iris TG 209C. The chemical functional groups present in the samples were determined by FTIR spectroscopy using Bruker Vector 22 in the range of wave numbers from 4000 to 400 cm^{-1}. Zeta potentials were measured (in triplicate) on a Zetaphorometer IV (CAD Instruments).

II.4 Adsorption tests

Batch adsorption experiments were conducted in order to evaluate the selectivity of different materials. Effect of solution pH, contact time and initial dyes concentration were investigated. All experiments were conducted at room temperature and the stirring speed was maintained at 150 rpm. After reaching equilibrium, the mixture was filtered by syringe filter (0.20 µm) and the dye filtrate was then analyzed using a UV–vis spectrophotometer (**Cary-Varian 60**) by measuring the absorbance at a wavelength corresponding to maximum absorbance of each dye.

II.5 Comparison of materials

Batch tests with NGB and RB solutions were used to compare the adsorption capacity of the parent materials (as-synthesized MCM-41) and its modified counterparts (DHA-41A, DHA-41B and DHA-41C). In a beaker, 100 mL of NGB or RB dye solution (initial concentration 100mg/L) was mixed with 100 mg of each adsorbent and then stirred at room temperature for 24 hours to ensure the adsorption equilibrium.

II.6 Effect of pH

The pH of aqueous solutions is a significant parameter for the removal of toxic compounds by adsorption because the pH value affects the structural properties of sorbents and analytes [15]. A mass of 20 mg of DHA-41 A or DHA-41 C was added to a series of flask containing 20mL of NGB or RB dye solution respectively, at concentration 100mg/L. The pH of dye solutions was adjusted to a pH range from 2 to12 using diluted hydrochloric acid (0.1 M) and sodium hydroxide solutions (0.1

M) and measured by EUTECH Instrument (Ecoscan pH5) pH meter.

II.7 Kinetic study

The kinetic study was accomplished with suspensions of DHA-41A (20 mg) in 20mL of NGB dye solution (100 mg/L). The mixtures were stirred during different time intervals, ranging from 5 to 240 min and then filtered. The supernatant was determined using a UV-visible spectrophotometer at wave length of NGB dye. The same procedure was used for the kinetic sorption study of the

$$Ln(q_e - q_t) = Lnq_e - \frac{k_1}{2.303}t \quad \text{.....(1)}$$

Where q_e is the equilibrium adsorption amount, q_t the adsorption amount at time t and k_1 is the pseudo-first order rate constant.

The linear form of pseudo-first order model can be expressed as follow:

$$\frac{t}{q_t} = \frac{1}{k_2 * q_e^2} - \frac{t}{q_e} \quad \text{.....(2)}$$

Where q_e is the equilibrium adsorption amount, q_t the adsorption amount at time t and k_2 is the pseudo-second order rate constant.

Since the diffusion mechanism cannot be differentiated by the pseudo-first and -second order models, the Weber and Morris equation was further employed to calculate the rate constants of intraparticle diffusion [20]. The equation for intraparticle diffusion is given by:

$$q_t = k_{id} * \sqrt{t} + l \quad \text{.....(3)}$$

where k_{id} is the rate constant and the l value is associated with the thickness of the boundary layer.

II.8 Adsorption experiments

For adsorption experiments, 20 mg of DHA-41A samples were added into 20 ml of NGB solution at the desired concentration (from 10mg/L to 1000mg/L). The solution was stirred for about 90 min and 20°C, for the sorption process to reach equilibrium. The same procedure was used for the adsorption experiments study of the cationic dye RB, with suspensions of DHA-41C, (20 mg) in 20mL of cationic dye solutions (from 10mg/L to 1000mg/L).

After contact, the content of the flasks were filtered with a syringe filter to collect the final solutions, then the residual concentration was measured by using UV–vis spectrophotometer at 554 and 714 nm for RB and NGB respectively.

III. Results and discussion

III.1Characterization of adsorbents

The nitrogen adsorption–desorption isotherms of parent material MCM-41P and its modified counterparts are presented in Fig.1. Each sample shows type IV isotherm according to the IUPAC classification with H1 hysteresis loops which are representing mesoporous for the expanded materials DHA-41A, DHA-41A B and DHA-41A C. The non-expanded samples exhibited a reversible adsorption–desorption isotherms with the characteristic nitrogen condensation and evaporation steps of mesoporous materials with narrow pore size distributions [21, 22]. Similarly, DHA-41C exhibits a type IV isotherm with a broad H1 hysteresis loop occurring at higher relative pressure, which confirms the pore enlargement. This is consistent with the narrow pore size distribution shown in Fig.2. The BET surface area, pore volume and average pore sizes of different samples are listed in Table.1. The average pore size was taken as the peak of the pore size distributions as calculated from the adsorption branch using the KJS (Kruk–Jaroniec–Sayari) method,

The total pore volume was determined as the volume of liquid nitrogen adsorbed at P/P_0 of 0.995. From this table it is clearly shown that the parent material (MCM-41P) has a large specific surface area (1207 m^2/g), which gradually decreases during post-synthesis and extraction treatment confirming the pore blockage by amine moieties. However, the carbonized material (DHA-41C) showed the highest value of the specific surface area (1237 m^2/g) due to the release of pores of MCM-41 during heat treatment. The value of the pore diameter and the pore volume increased significantly after the different treatments, except for the DHA-41A, [23] which had a low pore volume strongly due to the higher content of the amine moieties found inside the pores.

The XRD patterns of all samples at low-angle are presented in **Fig.3**. All samples show an intense peak (100) and three low intensity peaks (110), (200), and (210) that are characteristic of hexagonal mesoporous silica of MCM-41. The modified samples showed the presence of all peaks characteristic of the mesoporous silica MCM-41 with a slight decrease; this also shows that the structure of the MCM-41 was maintained after the cationic dye with suspensions of DHA-41C, (20 mg) in 20mL of RB dye solution (100 mg/L). The sorbed amounts were determined from the difference between the initial and final concentrations.

The adsorption process can be described by either pseudo-first order,[16] or pseudo-second order kinetics [17].

The linear form of pseudo-first order model can be expressed as follow [18, 19]:

different treatments. The diffraction peaks of modified materials shift to the lower 2θ values as a consequence of the swelling effect. Table 2 shows the evolution of the lattice parameter a_0 during the different treatments. It is clearly indicated that the lattice parameter a_0 was increased during post-treatment by DHA which caused the swelling of the pores of MCM-41. These results are similar to the literature [24].).

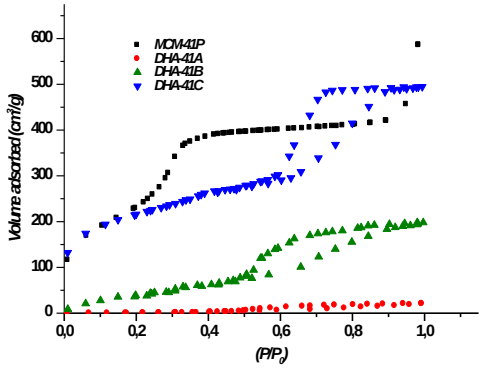

Fig 1. *Nitrogen adsorption-desorption isotherms of different adsorbents*

Table 1. *Structural and textural properties of MCM-41 and its modified counterparts*

Samples	a_0 (nm)[a]	S_{BET} (m^2/g)	d_P (nm)	V_P (cm^3/g)
MCM-41	4.47	1207	3.42	0.85
DHA-41A	5.07	167	6.05	0.255
DHA-41B	4.86	382	5.92	1.04
DHA-41C	5.17	1237	12.46	1.89

[a] Lattice parameter calculated from d_{100} using both equation, $d_{100}=\lambda/2sin\,\Theta$ and $a_0=2d_{100}/\sqrt{3}$

[b] Average pore diameter determined from the strongest peak of the distribution of BJH

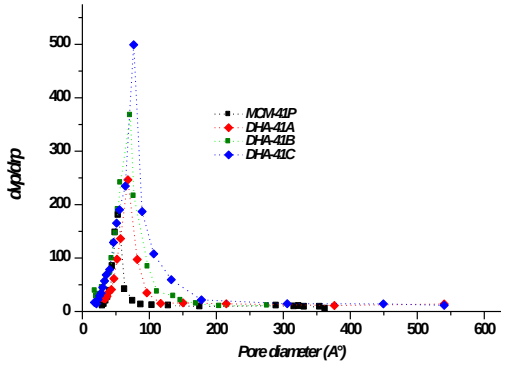

Fig 2. *BJH-pore size distribution of different adsorbents.*

Extraction of DHA from the sample DHA-41A using ethanol as solvent leads to the slight decrease in the lattice parameter probably due to the presence of some DHA molecules in the structure of MCM-41, while the carbonization of sample DHA-41A slightly increases the lattice parameter from 5.07 nm to 5.17 nm (DHA-41CThe parent material MCM-41P and its counterparts modified by different treatments were also examined by infrared spectroscopy FTIR as shown in **Fig. 4**. All samples presented vibration bands at 1244, 1081, 796 and 457 cm^{-1} attributed to Si–O–Si bands of condensed silica network. The peak around 1637cm^{-1} is assigned to the bending vibration of adsorbed water. The vibration band of Si–OH decrease around 958cm^{-1}, after pore expanding of synthesized materials due to the interaction between $–NH_2$ groups and the silanol groups through hydrogen bending; [25]. The bands corresponding to the C– H stretching and bending vibrations appear in 2923 and 2857 cm^{-1}; these peaks became intense in all materials containing amine groups. The presence of bands in 690, 1460 and 2937 cm-1 is assigned to N–H bending vibration, N–H asymmetric bending vibration and C–H link, respectively [26]. The bands of C–N stretching vibration is normally observed around 1000–1200 cm^{-1} which also overlaps with the vibrations of the Si-O-Si bond [27]

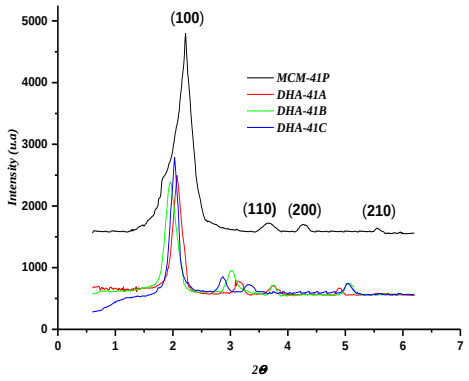

Fig 3. *XRD patterns of parent material MCM-41 and its modified counterparts*

. The presence of bands in 690, 1460 and 2937 cm-1 is assigned to N–H bending vibration, N–H asymmetric bending vibration and C–H link, respectively [26]. The bands of C–N stretching vibration is normally observed around 1000–1200 cm^{-1} which also overlaps with the vibrations of the Si-O-Si bond [27].

Thermogravimetric analyses of parent material MCM-41P and its modified counterparts are shown in **Fig.5 (a and b)**. According to the TGA and dTG profiles, it is found that all samples have two mass losses due to the dehydration and degradation of the water and the organic matter respectively. The first mass loss occurs between 30-150 °C, in which the water mass loss varies between 7-22%. The material DHA-41B showed the highest hydrophilic character strongly due to the several interactions between the water molecules and amine groups and

also to the free silanol groups. It should also be noted that this material (DHA-41B) showed higher water affinity compared to its counterpart DHA-41A.

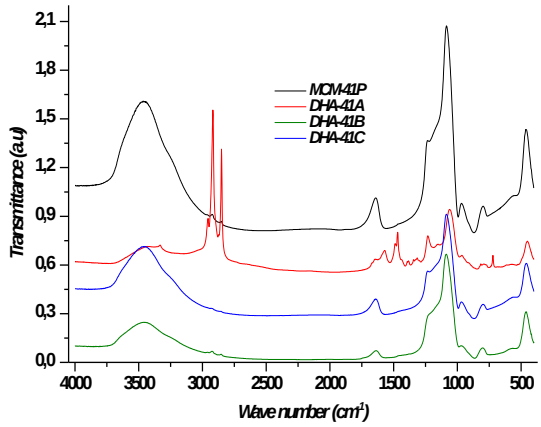

Fig 4. *FTIR spectra of as-synthesized MCM-41 P and its modified counterparts*

These results confirm our hypotheses proposed in the XRD and nitrogen adsorption-desorption analysis. DHA-41C material showed a low weight loss of organic matter (almost negligible) which was removed during the carbonization treatment. Above 600 °C, all samples exhibit about ~1% of mass loss due to the dehydroxylation of the silicate networks [29].

Zeta potentials of the all samples were measured in a wide pH range to identify isoelectric points. As shown in **Fig.6**, the results indicate that the pH_{PZC} of the different samples varies in the following sequence; 3.84, 6.14, 9.25, 4.64 for DHA-41C, MCM-41P, DHA-41A and DHA-41B respectively. For example, DHA-41A have a positive charge at pH< $pH_{PZC(A)}$ = 9.25, this can be attributed to the amine groups and the quaternization of surface containing CTAB/DHA. These results also provide an indirect evidence of the existence of cationic groups on DHA-41A, thus altering the surfacechemistry of the materials. For DHA-41C, the results showed that the material present negative charges throughout the pH > $pH_{PZC(C)}$ = 3.84. From this result, we can conclude that the materials DHA-41A can be used an excellent adsorbent for negatively charged species and DHA-41C for positively charged species

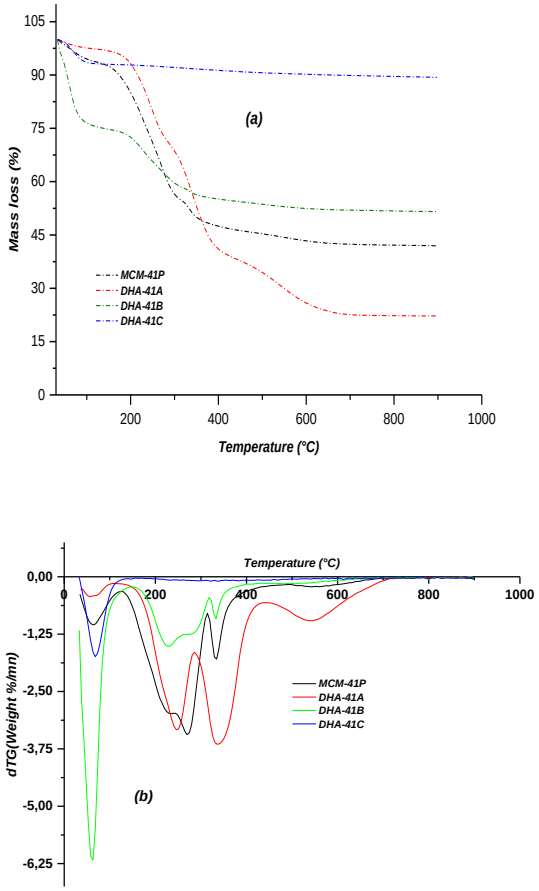

Fig 5. *Thermogravimetric analysis of parent material MCM-41P and its modified counterparts,* ***(a)*** *TGA and* ***(b)*** *dTG profiles*

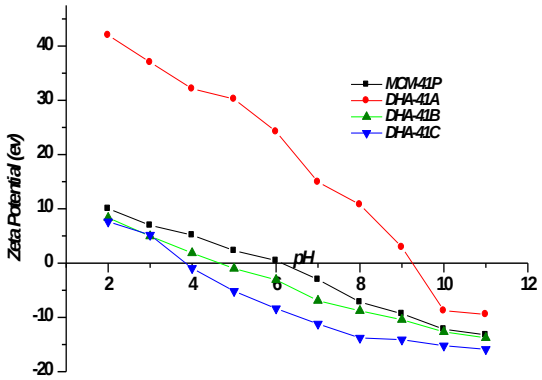

Fig 6. *Zeta potentials vs. pH for the MCM-41 P, DHA-41A, DHA-41 B and DHA-41C*

III.2. Adsorptions experiments:

III.2.1. Comparison of Materials

Batch tests with anionic and cationic dyes solutions were used to compare the adsorption capacity of parent material MCM-41P and its modified counterparts (see **Fig.7**). Adsorption of the anionic dye on DHA-41A was significantly enhanced in compared to the others samples. The adsorbed amounts of NGB dye were 33.31, 97.82, 77.66 and 17.18% for MCM-41P, DHA-41A, DHA- 41B and DHA-41C, respectively. This affinity via the NGB dye was strongly related to the surface of the sample DHA-41A which is the most positively charged allowing it a strong interaction with anionic NGB dye, while the best adsorption capacity of cationic RB dye was obtained by the carbonized material DHA-41C due to its negative surface. The adsorbed amounts of RB dye were 24.81, 16.59, 44.25 and 93.94% for MCM-41P, DHA-41A, DHA-41B and DHA-41C, respectively.

III.2.2. Effect of pH

The solution pH is one of the most important factors, which influence the adsorption behavior. The variation in pH can influence the surface charge and the degree of ionization of the adsorbents [30].

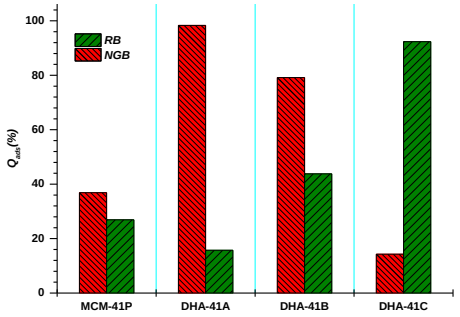

Fig 7. *Effect of the adsorbent nature on the adsorption capacity of RB and NGB dyes*

In this study, the effect of initial pH on adsorption capacity was studied in the range 2–12 at an initial dyes concentration of 100 mg/L. **Fig.8**. Shows effect of pH on the adsorption capacity of both dyes obtained from DHA-41A and DHA-41C. One can see that the adsorption capacity of the NGB dye was affected slightly by the pH ranging from 2 to 9 and the average adsorption capacity was 96.93mg/g. As known NGB is an acid dye and also called anionic dye [31].Therefore, at pH < pHpzc of DHA-41A (9.25), the DHA-41A surface will be positively charged, which increases the electrostatic attractions between acid dye molecules and DHA-41A surface. At higher pH values (pH >9) the number of positively charged sites are reduced and raised the number of negatively charged sites, creating electrostatic repulsion between the negatively charged surface of the DHA-41A and the anionic acid dye molecules. As a result, there was in a significant reduction in the adsorption of acid dye from the solution. A similar behavior was observed for the adsorption of anionic dyes onto amino-functionalized nanoporous silica SBA-3 and MCM-41, [1, 32]. For the RB dye, we can see that the adsorption capacity decreases significantly at low (2-4) and high pH > 9 pHs. However it did not very much in range of pH value from 4 to 9. Lower adsorption of RB dye in the acidic pH range is probably due to the presence of excess H^+ ions competing with the cation groups on the dye for adsorption sites [33].

Furthermore, a reported pHpzc value for DHA-41C is 3.84. At pH values lower than the corresponding pHpzc value of the adsorbent DHA-41C, have a net positive charge. Thus, the adsorbent tends to oppose the adsorption of the cationic dye. At pH values higher than the corresponding pHpzc value of the adsorbent, the surface of DHA-41C tends to acquire negative charge, thereby resulting in an increased adsorption of cationic dye due to increasing electrostatic attractions between the positively charged functional groups located on the basic dye and the negatively charged surfaces of the adsorbents. Similar observations were previously reported for the adsorption of methylene blue **[**34, 35**]** and Basic Yellow 87 [36]. On the other hand, the obvious decrease in the adsorption capacity of anionic and cationic dyes at high pH may be due to the decrease in the structure stability of the MCM-41 (such as the dissolution of MCM-41 in basic solution) [34]

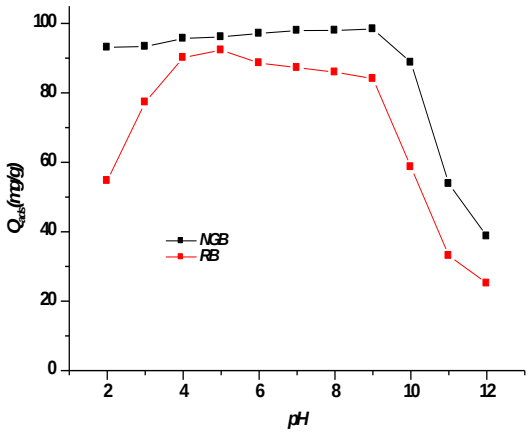

Fig 8. *Effect of pH on the adsorption of both dyes obtained from DHA-41A and DHA-41C.*

III.2.3 Kinetic

The adsorption experiments were carried out for different contact times with fixed adsorbent dose and concentration. Fig.9. presents graphs for the variation in adsorption with respect to time of NGB and RB at room temperature and indicates that the

adsorption gradually increases with increase in contact time. For both dyes, initially the adsorption of dye increases with increasing contact time and rate of adsorption becomes lower after 50 min. However, the maximum adsorption was achieved after 60 and 90 min for RB and NGB, respectively.

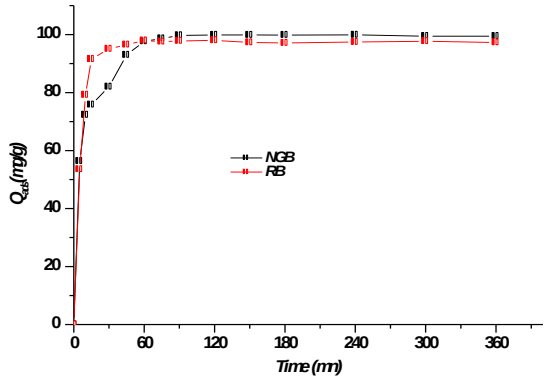

Fig 9. *Effect of contact time on NGB and RB adsorption onto DHA-41 A and DHA-41 C, respectively*

Linear arrangements Eqs (1) and (2), are commonly used to check the validity of these models with the corresponding plots. By contrasting the values of coefficient of determination (R^2), it was found that the pseudo-second order kinetic model fitted better with kinetic data of adsorbent DHA-41A (NGB) and DHA-41C (RB) than pseudo-first order kinetic model. In Fig. 10, a plot of Q_{ads} versus $t^{1/2}$ is presented for adsorption of NGB and RB onto DHA-41 A and DHA-41C, respectively. The examination of Fig. 10 indicates that the curves are not linear for all range of concentration studied, For NGB and RB dyes, two stages of different slopes was observed for all the concentrations, indicating that the diffusion intraparticle is not the only stage limiting speed, but other processes can be implied in the process of adsorption [37].

Kinetic parameters for the adsorption of NGB onto DHA-41A and RB onto DHA-41C are listed in **Table.2**.

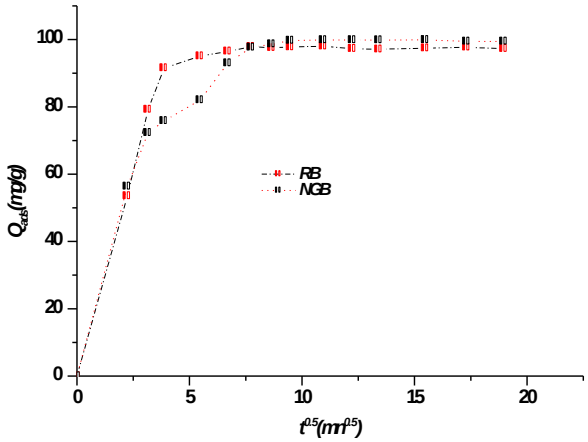

Fig 10. *Plots of intra-particle diffusion model for the adsorption of NGB and RB adsorption onto DHA-41 A and DHA-41 C, respectivel*

Table 2. *Parameters of kinetic model of NGB and RB adsorption onto DHA-41A and DHA-41C respectively.*

Material	**Pseudo - first order**			**Pseudo - second order**			**Intra-particule diffusion**		
	k_1 (min^{-1})	Q_e (mg/g)	R^2	k_2 ($g.min^{-1}.mg^{-1}$)	Q_e (mg/g)	R^2	k_{id} ($min^{-0.5}$)	l	R^2
DHA-41A « NGB »	$1.1.10^{-2}$	39.14	0.89	$3.8.10^{-3}$	104.52	0.99	12.15	30.61	0.95
DHA-41C « RB »	$2.9.10^{-2}$	28.77	0.84	$9.5.10^{-3}$	98.73	0.99	1.61	45.84	0.97

III.2.4Adsorption isotherms

Adsorption isotherm models can describe the interaction of a sorbent with a given adsorbate which is essential for its effective application. In this work data for adsorption isotherms were obtained after equilibrium time was reached at a given pH for each dye. Adsorption capacities (q_e) are expressed as mg of adsorbed dye per mass unit of sorbent (mg/g) and determined as follows:

$$q_e = (C_0 - C_e) * \frac{V}{m} \quad \ldots\ldots\ldots\ldots\ldots\ldots\ldots\ldots\ldots\ldots (4)$$

Where C_0 and C_e are the initial and the equilibrium dye concentrations of the solution, respectively

(mg/L), V is volume of solution (L) and m is the adsorbent mass (g).Langmuir, Freundlich and Sips isotherms models were used to describe the relationship between the amount of adsorbate adsorbed on the adsorbent and the concentration of dissolved adsorbate in the liquid at equilibrium. Langmuir, Freundlich and Sips adsorption isotherms can be expressed using Eqs. (5), (6) and 7), respectively [38]:

$$q_e = q_m * \frac{K_L * C_e}{(1 + K_L * C_e)} \quad \text{.....(5)}$$

$$q_e = K_F * C_e^{1/n} \quad \text{.....(6)}$$

$$q_e = q_m * \frac{(K_S * C_e)^{1/s}}{(1 + K_S * C_e)^{1/s}} \quad \text{.....(7)}$$

Where K_L and K_S are the adsorption equilibrium constant (L/mg), q_m is the maximum adsorption capacity (mg/g), (1/s) is the heterogeneity factor, K_F and (*1/n*) are arbitrary parameters. The dimension of K_F depends on the value of *1/n*.

The adsorption isotherms are shown in Fig.11 where Langmuir, Freundlich and Sips plots are represented. The maximum monolayer concentration of NGB and RB on different adsorbents reported elsewhere were also compared with the present study and tabulated in Table 3.

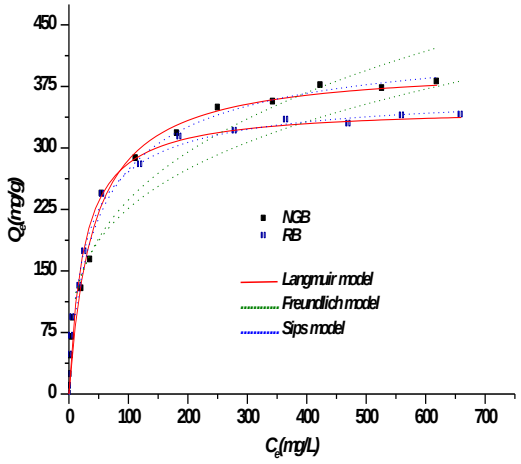

Fig 11. *Langmuir, Freundlich and Sips adsorption isotherms of NGB and RB onto DHA-41A and DHA-41 C, respectively*

The calculated parameters of Langmuir, Freundlich and Sips isotherms for the adsorption of NGB and RB onto DHA-41A and DHA-41C respectively were being listed in Table 4. It is evident from these data that the adsorption NGB and RB onto DHA-41A and DHA-41C samples was fitted well to all of the isotherm models as indicated by the R^2 values in **Table 3.**

Based on the Langmuir isotherm, the maximum adsorption capacities (q_m) of the used samples were 444.55 mg/g for NGB and 372.59 mg/g for RB. In this study, the q_m values of DHA-41A for NGB and DHA-41C for RB were compared with other results reported in literature, **Table 4.** It should be noted functionnalized DHA-41A is considered as good adsorbent NGB and DHA-41C for RB.

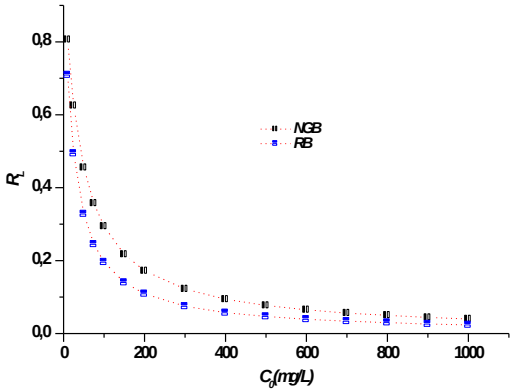

Fig 12. *R_L values versus the initial concentration of NGB and RB.*

Moreover, all of the calculated heterogeneity factors of 1/s are roughly close to 1.0, and the Sips model could be further reduced to the Langmuir equation in this case. This result indicated that DHA-41A and DHA-41C are both homogenous adsorbents and represent monolayer adsorption of the two dyes. The dimensionless constant separation factor, R_L, which is an indicator of the adsorption capacity, can be defined by the following equation:

$$R_L = \frac{1}{(1 + K_L * C_0)} \quad \text{.....(8)}$$

Table 3 . *Adsorption isotherm parameters for the adsorption of NGB and RB onto DHA-41A and DHA-41 C, respectively*

Material	Langmuir			Freundlich			Sips (Langmuir-Freundlich)			
	Q_{max} (mg/g)	K_L (L/g)	R^2	K_F (L/g)	1/n	R^2	Q_{max} (mg/g)	K_S (L/g)	1/s	R^2
DHA-41A NGB	401.21	0.024	0.996	54.76	0.317	0.945	**444.55**	0.044	0.918	0.993
DHA-41C RB	349.67	0.041	0.997	63.19	0.277	0.937	**372.59**	0.065	0.942	0.994

where C_0 (mg/L) is the initial dye concentration in aqueous solution. The adsorption process is considered favorable when $0 < R_L < 1$ and unfavorable when $R_L > 1$.

Fig.12. represents the calculated R_L values versus the initial concentration of anionic and cationic dyes at room temperature. All the calculated R_L values were between 0 and 1, indicating that the adsorption of anionic dyes onto DHA-41A and cationic dyes onto DHA-41C were favorable at the conditions being studied.

For DHA-41A/NGB $0.041 < R_L < 0.806$

For DHA-41C/RB $0.024 < R_L < 0.709$

Table 4. *Comparison of adsorption capacities of NGB and RB onto various adsorbents*

Adsorbent	q_{max} (mg/g)	Reference
For Naphtol Green B		
Regenerated commercial activated carbon WD-extra	97.0	[39]
Calcined Layered Double Hydroxides	193.4	[40]
Metal hydroxides sludge	10.0	[31]
(Zn - S: Cu - NPs - PAC).	75,70	[41]
DHA-41A	**444.55**	This work
For Rhodamine B		
Kaolinite	46.1	[42]
Porous carbon	479.0	[43]
Bagasse pith	263.85	[44]
Organo-vermiculites	281.0	[45]
DHA-41C	**372.59**	This work

IV. Conclusion

Ordered hexagonal materials (MCM-41) was successfully modified by post-synthesis using alkyl amine (DHA), the amine was extracted with soxhlet by ethanol and dried at ambient conditions at the end aminated and/or desaminated material was carbonized. All materials were characterized and investigated as adsorbents for the removal of two dyes Naphtol Green B and Rhodamine B from aqueous solutions. The hexagonal structure of MCM-41 remains intact after the different modifications. The XRD results showed that the modification of the MCM-41 by DHA led to the inflation of the mesh. DHA-41A has a strong hydrophilic character compared to other materials that allow the transport of water-soluble species. DHA-41B containing only CTAB surfactant, exhibited a wide open pore structure which can be used in adsorption of hydrophobic molecules. DHA-41C exhibited highly enlarged pores with relatively narrow size distribution with a diameter of 77 Å. FT-IR spectra confirm the incorporation of amine moieties in mesoporous silica MCM-41 structure. It was demonstrated that the adsorption of the anionic dye was enhanced using DHA-41A, whereas adsorption of cationic dye was enhanced by DHA-41C. Moreover, the calculated q_e values also agree with the experimental data in the case of pseudo-second-order model. The Langmuir, Freundlich and Sips isotherm models were used to describe adsorption data. The equilibrium data fit well in the Langmuir model of adsorption.

The adsorption of the two dyes is favorable because the dimensionless constant separation factor, R_L is between 0 and 1; this adsorption is more favorable at low concentrations until the arbitrary parameter (1 / n) of Freundlich is less than 1.

The values very close to 1 of the Sips heterogeneity factor (1 / s) confirm that the surface of DHA-41A and DHA-41C are homogeneous.

V. References

1. Anbia, M. ; Salehi, S. Removal of acid dyes from aqueous media by adsorption onto amino functionalized nanoporous silica SBA-3, *Dyes Pigments* 94 (2012) 1–9.
2. Hassaan, M. ; El Nemr, A. ; Hassaan, A. MHealth and environmental impacts of dyes: mini review, *American Journal of Environnemental Science and Engineering*. 1 [2017] 64–67.
3. Benkhaya, S. ; El Harfi, S. ; El Harfi, A. Classifications, properties and applications of textile dyes, a review. *Applied Journal of Environmental Engineering Science* 3 (2017) 311–320.
4. El-Naggar, M. E. ; Radwan, E. K. ; El-Wakeel, S. T. ; Kafafy, H. ; Gad-Allah, T. A. ; El-Kalliny, A. S. ; Shaheen, T. I. Synthesis, characterization and adsorption properties of microcrystalline cellulose based nanogel for dyes and heavy metals removal. *International Journal of Biological Macromolecules* 113 (2018), 248–258.
5. Badawi, M. A. ; Negm, N. A. ; Abou Kana, M. T. H. ; Hefni, H. H. ; Abdel Moneem, M. M, L. Adsorption of aluminum and lead from wastewater by chitosan-tannic acid modified biopolymers: Isotherms, kinetics, thermodynamics and process mechanism, *International Journal of Biological Macromolecules* 99 (2017) 465-476.
6. Galán, J. ; Rodríguez, A. ; Gómez. J. M.. Allen, S. J. ; Walker, G. M. Reactive dye adsorption onto a

novel mesoporous carbon. *Chemical Engineering Journal*, 219 (2013) 62-68.

7. Cashin, V.B. ; Eldridge, D.S. ; Yu, A. ; Zhao, D. Surface functionalization and manipulation of mesoporous silica adsorbents for improved removal of pollutants: a review, *Environmental Science*: *Water Research* & *Technology* 4 (2018) 110–128.
8. Yokoi, T.; Tatsumi, T.; Yoshitake, H. Fe^{3+} coordinated to amino-functionalized MCM-41: an adsorbent for the toxic oxyanions with high capacity, resistibility to inhibiting anions, and reusability after a simple treatment. *Journal of Colloid Interface Science.* 274 (2004) 451–457.
9. Saad, R.; Belkacemi, K.; Hamoudi, S. Adsorption of phosphate and nitrate anions on ammonium-functionalized MCM-48: effects of experimental conditions. *Journal of Colloid Interface Science* 311 (2007) 375–381.
10. Santos, D.O. ; Santos, M.L.N. ; Costa, J.A.S. ; Anjos de Jesus, R. ; Navickiene, S. ; Sussuchi, E.M. ; Eliane de Mesquita, M. Investigating the potential of functionalized MCM-41 on adsorption of Remazol Red dye, *Environmental Science Pollution Research*. 20 (2013) 5028–5035.
11. Sayari, A. ; Yang, Y. Highly Ordered MCM-41 Silica Prepared in the Presence of Decyltrimethylammonium Bromide. *Journal of Physical Chemistry B.* 104 (2000) 4835–4839.
12. 12. Benhamou, A. ; Baudu, M. ; Derriche, Z. ; Basly, J.P. Aqueous heavy metals removal on amine functionalized Si-MCM-41 and Si-MCM-48. *Journal of Hazardous Material*. 171 (2009) 1001–1008.
13. Kruk, M. ; Jaroniec, M. ; Sayari, A. Application of Large Pore MCM-41 Molecular Sieves To Improve Pore Size Analysis Using Nitrogen Adsorption Measurements. *Langmuir* 13 (1997) 6267–6273.
14. Barrett, E. P. ; Joyner, L. G. ; Halenda, P. P. The determination of pore volume and area distributions in porous substances. I. computations from Nitrogen Isotherms. *Journal of American Chemistry Society*. 731 (1951) 373-380.
15. Donmez, G.; Aksu, Z. Removal of chromium (VI) from saline wastewaters by Dunaliella species. *Process Biochemistry*. 38 (2002) 751–762.
16. Lagergren, S. About the theory of the so-called adsorption of soluble substances, Kungliga Svenska Vetenskapsakademius. *Hadndlingar* 24 (1898) 1–39.
17. Ho, Y.S. ; McKay, G. Kinetic model for lead (II) sorption on peat. Adsorption. Science and Technology 16 (4) (1998) 243–255.
18. 18. Tsai, C.H. ; Chang, W.C. ; Saikia, D. ; Wu, C.E. ; Kao, H.M. Functionalization of cubic mesoporous silica SBA-16 with carboxylic acid via one-pot synthesis route for effective removal of cationic dyes. *Journal of Hazardous Material*. 309 (2016) 236-248.
19. Wu, Y. ; Qi, H. ; Li, B. ; Huang, Z. ; Li, W. ; Liu, S. Novel hydrophobic cotton fibers adsorbent for the removal of nitrobenzene in aqueous solution, Carbohydrate Polymers 155 (2017) 294–302.
20. Weber, W.J. ; Morris, J.C. Intraparticle diffusion during the sorption of surfactants onto activated carbon, *Journal of the Sanitary Engineering Division* 89 (1963) 31–6
21. Kresge, C. T.; Leonowicz, M. E.; Roth, W. J.; Vartuli, J. C.; Beck, J. S. Ordered mesoporous molecular sieves synthesized by a liquid-crystal template mechanism. *Natur*e, 359 (1992) 710- 712.
22. Zhao, X. S. Lu, G.; Hu, X. Organophilicity of MCM-41 adsorbents studied by adsorption and temperature-programmed desorption. *Colloids Surface. A*, 179 (2001) 261-269.
23. Loganathan, S.; Tikmani, M.; Mishra, A.; Ghoshal, A. K. Amine tethered pore-expanded MCM-41 for CO_2 capture: Experimental, isotherm and kinetic modeling studies. *Chemical Engineering Journal* 303 (2016) 89–99.
24. Laghaei, M.; Sadeghi, M.; Ghalei, B.; Dinari,M. The effect of various types of post-synthetic modifications on thestructure and properties of MCM-41 mesoporous silica, *Progress in Organic Coatings* 90 (2016) 163–170.
25. Sartori, G.; Bigi, F.; Maggi, R.; Sartorio, R.; Macquarrie, D.J.; Lenarda, M.; Storano, L.; Coluccia, S.; Martra, G. Catalytic activity of aminopropyl xerogels in the selective synthesis of (E) nitrostyrenes from nitroalkanes and aromatic aldehydes. *Journal of Catalysis* 222 (2) (2004) 410–418.
26. Li J, Miao X.; Hao Y.; Zhao J.; Sun X.; Wang L. Synthesis, amino-functionalization of mesoporous silica and its adsorption of Cr(VI). *Journal Colloid Interface Science* 318(2) (2008) 309–314.
27. Shriner R.L.; Hermann . C.K.F.; Morrill T.C.; Curtin D.Y.; Fuson R.C. Systematic Identification of Organic Compounds (seventh ed.), *Wiley*, New York (1998), 324.
28. Wang, Y.; Mu, Y.; Zhao, Q. B. Isotherms, kinetics and thermodynamics of dye biosorption by anaerobic sludge, *Separation and Purification Technology* 50 (2006) 1–7.
29. Zhao, X.S.; Lu,G.Q., Whittaker, A.K.; Millar, G.J.; Zhu, H.Y. Comprehensive study of surface chemistry of MCM-41 using 29SiCP/MAS NMR, FTIR, pyridine-TPD and TGA, *Journal of Physical Chemistry B* 101 (33) (1997) 6525–6531.
30. 30. Zhou, Y.; Lu, J.; Zhou, Y.; Liu, Y. Recent advances for dyes removal using novel adsorbents: A review. *Environmental Pollution* 252 (2019) 352-365.
31. Attallah, M.F.; Ahmed, I.M.; Hamed, M.M. Treatment of industrial wastewater containing congo red and naphthol green B using low-cost adsorbent. *Environmental Science Pollution Research.* 20 (2013) 1106–1116.
32. Qin, Q.; Ma, J.; Liu,K. Adsorption of anionic dyes on ammonium-functionalized MCM-41, *Journal of Hazardous Material*s 162 (2009) 133–139.
33. Sharma, Y. C. Adsorption Characteristics of a Low-Cost Activated Carbon for the Reclamation of Colored Effluents Containing Malachite Green. *Journal of Chemical Engineering. Data* 56 (2011) 478–484.
34. Juang, L. C.; Wang, C.C.; Lee, C. K. Adsorption of basic dyes onto MCM-41, *Chemosphere* 64 (2006) 1920–1928.
35. Lee, C.; Liu, S.S.; .Juang, L.C.; Wang, C.C.; Lin, K.S.; Lyu, M.D. Application of MCM-41 for dyes removal from wastewater. *Journal of Hazardous Materials* 147 (2007) 997–1005.
36. Wu, X.; Hui, K. N.; Hui, K.S.; Lee, S.K.; Zhou, W.; Chen, R.; Hwang, D. H.; Cho, Y. R.; Son, Y.G. Adsorption of basic yellow 87 from aqueous solution onto two different mesoporous adsorbents, *Chemical Engineering Journal* 180 (2012) 91-98.
37. Oussalah, A.; Boukerroui, A.; Aichour, A.; Djellouli,B. Cationic and anionic dyes removal by low-cost hybrid alginate/natural bentonite composite beads: Adsorption and reusability studie. *International Journal of Biological Macromolecules* 124 (2019) 854–862.
38. Laaz, I.; Stébé, M. J.; Benhamou, A.; Derriche Z.; Blin, J. L. Influence of porosity and surface modification on the adsorption ofboth cationic and anionic dyes. *Colloids and Surfaces A: Physicochemical Engineering Aspect*s 490 (2016) 30–40.
39. Adamczyk, D.; Bezak-Mazur, E. Regeneration of WD-extra activated Carbon spent in Acid Dyes adsorption Process by Fenton's Reagent, *Advanced Research in Scientific Areas* 7 (2012) 1408 – 1411.
40. Zhang, F.; Ni, Z.; Xia, S.; Liu,X.; Wang, Q. Removal of Naphthol Green B from Aqueous

Solution by Calcined Layered Double Hydroxides: Adsorption Property and Mechanism Studies, *Chinese Journal of Chemistry*. 27-9 (2009) 1767–1772.

41. Masoudian, N.; Rajabi,M.; Ghaedi, M.; Asghari. A Highly efficient adsorption of Naphthol Green B and Phenol Red dye by Combination of Ultrasound wave and Copper-Doped Zinc Sulfide Nanoparticles Loaded on Pistachio-NutShell. *Applied Organometallic Chemistry* e4369 (2018) 1-13.
42. Khan, T.A.; Dahiya, S.;. Ali, I. Use of kaolinite as adsorbent: Equilibrium, dynamics and thermodynamic studies on the adsorption of Rhodamine B from aqueous solution. *Applied Clay Science* 69 (2012) 58–66.
43. Guo, Y. P, Zhao, J.Z, Zhang, H, Yang, S.F, Qi, J, Wang, Z, Xu, H.D, Use of rice huskbased porous carbon for adsorption of rhodamine B from aqueous solutions, Dyes Pigments 66 (2005) 123–128.
44. Gad, H.M.H. ; El-Sayed, A.A. Activated carbon from agricultural by-products for the removal of rhodamine B from aqueous solution. *Journal of Hazardous Materials* 168 (2009) 1070–1081.
45. Yu, M. ; Gao, M. ; Shen, T. ; Zeng, H. Single and simultaneous adsorption of rhodamine B and congo red from aqueous solution by organo-vermiculites. *Journal of Molecular Liquids 292* (2019) 111408.

Please cite this Article as:
Barca A., Benhamou A., Benyoub N., Debab A., Functionalized mesoporous silica materials for dyes adsorption**,** ***Algerian J. Env. Sc. Technology****, 7*:4 **(2021) 2190- 2200**